Research Square

Preprints are preliminary reports that have not undergone peer review.
They should not be considered conclusive, used to inform clinical practice,
or referenced by the media as validated information.

# Draft genome analysis and in vitro evaluation of probiotic-associated properties in Lacticaseibacillus paracasei UCO-100

**Víctor Fuentes-Barrera**
University of Concepción
**Cristobal Goic**
University of Concepción
**Cristian Parra-Sepulveda**
University of Concepción
**Héctor Valdebenito-Navarrete**
University of Concepción
**Kimberly Sánchez-Alonzo**
University of Concepción
**Michel Abanto**
Universidad de La Frontera
**Apolinaria García-Cancino**
apgarcia@udec.cl
University of Concepción

**Article**

**Keywords:** Lacticaseibacillus paracasei, probiotic potential, whole-genome sequencing

**Posted Date:** September 8th, 2026

**DOI:** https://doi.org/10.21203/rs.3.rs-10679803/v1

**License:** This work is licensed under a Creative Commons Attribution 4.0 International License.
Read Full License

**Additional Declarations:** No competing interests reported.

## Abstract

Lactic acid bacteria (LAB) play important roles in industrial applications and provide beneficial effects to the host. Among them, *Lacticaseibacillus paracasei* exhibits characteristics associated with survival and colonization of the gastrointestinal tract. This study characterized the probiotic potential of *L. paracasei* UCO-100, isolated from the human gastric corpus, through genomic analysis and in vitro assays. Genomic analysis identified genes associated with gastrointestinal adhesion, exopolysaccharide biosynthesis, bacteriocin production, metabolic functions, and stress responses, as well as two putative RiPP-like bacteriocin biosynthetic gene clusters. *In vitro* assays showed tolerance to acidic pH and bile salts, 73.6% hydrophobicity, 54.3% autoaggregation, and high adhesion to abiotic surfaces. Safety assessment revealed no known acquired antimicrobial resistance genes or virulence genes were detected and no hemolytic activity. Mobile genetic elements were identified, but none carried antibiotic resistance or virulence genes. Overall, the genomic and phenotypic characteristics of *L. paracasei* UCO-100 support its potential as a probiotic strain and provide a basis for further investigation of its functional properties and potential probiotic applications.


## Introduction

Lactic acid bacteria (LAB) are a diverse group of microorganisms with important applications in food production, agriculture, industry, and clinical settings. Their relevance is largely attributed to their beneficial properties, including their role in fermentation processes, adaptability to different nutritional and environmental conditions, and adhesion capacity, which have facilitated their incorporation into a variety of matrices [1]. LAB are also common members of the human microbiota and inhabit several anatomical sites, including the oral cavity, gastrointestinal tract, respiratory mucosa, and skin, where they can contribute to host health [2]. Among LAB, several genera have attracted considerable attention, including *Lactobacillus*, *Lacticaseibacillus*, *Limosilactobacillus*, and *Lactiplantibacillus*. Species belonging to these genera have been extensively investigated for their potential health benefits and probiotic properties, including their relevance within a One Health context [3, 4].

Among these probiotic LAB, *Lacticaseibacillus paracasei*, previously classified as *Lactobacillus paracasei*, has gained particular interest due to its presence in the intestinal microbiota of healthy individuals and in a wide variety of fermented foods, including yogurt, kefir, and other dairy products [5, 6]. *L. paracasei* is a Gram-positive, facultatively heterofermentative bacterium that produces lactic acid as its major fermentation end product. Its cells typically range from 0.7 to 1.1 μm in width and from 2.0 to 4.0 μm in length, and its genomic G + C content ranges from 45% to 47%. Taxonomically, this species is closely related to *Lacticaseibacillus rhamnosus* [7].

The probiotic potential of *L. paracasei* has been widely investigated, particularly in relation to its ability to survive gastric acidity, colonize mucosal and intestinal environments, and provide health benefits such as enhancement of the immune response, improvement of digestion, and reduction of inflammation [8]. In this context, strains isolated from both fermented foods and human samples have been evaluated for their probiotic and functional properties. For instance, Bengoa et al. (2018) isolated *L. paracasei* strains

CIDCA 83123, CIDCA 83124, and CIDCA 8339 from kefir grains and demonstrated their ability to modulate the innate immune response of the intestinal epithelium [9]. Similarly, Romero et al. (2020) reported that *L. paracasei* CT12, isolated from Mexican kefir grains, exhibits antimicrobial and antioxidant properties [10].

Evidence of probiotic potential has also been reported for *L. paracasei* strains isolated from human samples. Strain NTU 101, isolated from human feces, together with its exopolysaccharide, exhibited antioxidant effects and modulated the macrophage response [11]. Likewise, *L. paracasei* 28.4, isolated from the oral cavity, was shown to exert antifungal activity against persistent fungal pathogens such as *Candida auris* [12]. Together, these findings highlight the functional diversity of *L. paracasei* strains obtained from different ecological niches and support the continued exploration of novel isolates with potential probiotic properties.

Based on this evidence, the present study aimed to characterize a novel *L. paracasei* strain isolated from a human gastric corpus biopsy by evaluating its main probiotic properties through both in vitro and in silico approaches. The characterization included the assessment of adhesion and autoaggregation capacity, stress response and tolerance to stress conditions, bacteriocin production, and safety, among other relevant parameters.

# Results

**General genomic characteristics of L. paracasei UCO-100.** Figure 1A shows the hybrid genome assembly of *L. paracasei* UCO-100. The assembled genome has a total size of 3,007,747 bp and consists of 61 contigs, with a GC content of 46.3%. A total of 2,949 genes were identified, including 2,873 coding sequences (CDSs), of which 2,798 correspond to protein-coding genes and 75 to pseudogenes. In addition, the genome contains 15 rRNA genes, 58 tRNA genes, and one CRISPR array. The main genomic characteristics of *L. paracasei* UCO-100 are summarized in Table 1. This Whole Genome Shotgun project has been deposited at DDBJ/ENA/GenBank under the accession JCANKF000000000. The version described in this paper is version JCANKF010000000.

**Phylogenetic relationship of L. paracasei UCO-100.** Figures 1B and 1C show the phylogenetic relationship of *L. paracasei* UCO-100. Average nucleotide identity (OrthoANIu) against 10 *L. paracasei* reference genomes ranged from 98.23% to 98.45%, including 98.44% against the type strain JCM 8130 (= ATCC 25302) (Fig. 1C). This was clearly discontinuous from the ANI observed against L. rhamnosus (77.1–77.8%), L. casei (77.1–78.4%), and L. zeae (77.1–77.9%), well below the 95–96% species boundary. A phylogenomic species tree inferred from 1,622 single-copy orthologous genes (OrthoFinder v2.5.5; STAG algorithm, STRIDE-rooted) placed UCO-100 within a well-supported *L. paracasei* clade (STAG support ≥ 0.96), clearly separated from the *L. rhamnosus* and *L. casei*/*L. zeae* clades (Fig. 1B).

**Prediction of bacteriocin biosynthetic gene clusters in L. paracasei UCO-100.** For *L. paracasei* UCO-100, two clusters predicted to be involved in bacteriocin biosynthesis (RiPP-like type) were identified using antiSMASH 8.0.4 under a “relaxed” detection criterion. These clusters are located in contig 8 (from position 1 to 11,428 bp) and contig 17 (from position 25,316 to 35,761 bp), as shown in Fig. 1D.

**Genomic information of L. paracasei UCO-100.** Functional genes were predicted in *L. paracasei* UCO-100 based on genome annotation using the Prokaryotic Genome Annotation Pipeline (PGAP). A total of 2,798 protein-coding sequences (CDSs) were analyzed across all contigs. Regarding probiotic properties, the predicted genes were classified into five functional categories: gastrointestinal tract adhesion, autoaggregation/EPS biosynthesis, bacteriocin production, enzyme production, and stress response. These findings are summarized in Table 2.

**Safety evaluation.** No genes conferring resistance to any of the antibiotics included in the panel defined for the *Lactobacillus casei/paracasei* group under EFSA guidance (ampicillin, chloramphenicol, clindamycin, erythromycin, gentamicin, kanamycin, streptomycin, and tetracycline; vancomycin is not required for this taxonomic group) were detected in the genome of *L. paracasei* UCO-100. Under the EFSA genomics-first framework, confirmatory phenotypic MIC testing is primarily required for antibiotics associated with acquired resistance genes. Since no acquired resistance genes were identified, phenotypic MIC testing was not performed for this strain (Table 3). Phenotypic antibiotic susceptibility was additionally assessed by disc diffusion (Table 5), which showed susceptibility to all tested antibiotics except bacitracin, a resistance commonly regarded as intrinsic and of no clinical relevance in lactobacilli. No virulence genes were detected either in the curated *Enterococcus*-associated panel (*gelE, hyl, asa1, esp, sprE, cylA, cytK, nhe*, and *hbl*) or in the complementary genome-wide screening against the Virulence Factor database (VFDB) core dataset. Furthermore, *L. paracasei* UCO-100 exhibited no hemolytic activity, corresponding to a γ-hemolytic phenotype (Table 3).

**Mobile genetic elements and genomic islands.** A total of three prophages, two insertion sequence (IS) clusters/transposons, and one genomic island were identified in the genome of *L. paracasei* UCO-100, whereas no integrative and conjugative elements (ICEs) were detected. None of these elements carried antibiotic resistance or virulence genes. Furthermore, no plasmid sequences were detected using PlasmidFinder. A Type II-A CRISPR-Cas system was identified on contig 3. These findings are summarized in Table 3.

Table 1
Genome assembly statistics of *L. paracasei* UCO-100. Correspond to the official NCBI Prokaryotic Genome Annotation Pipeline (PGAP).

| **Genome assembly statistics** | **Value** |
|---|---|
| Total length (bp) | 3,007,747 |
| Largest contig length (bp) | 470,112 |
| N50 length (bp) | 167,707 |
| Number of contigs | 61 |
| GC contents (%) | 46.3 |
| Genes (total) | 2,949 |
| CDSs (total) | 2,873 |
| CDSs (with protein) | 2,798 |
| Pseudogenes (total) | 75 |
| rRNAs (5S, 16S, 23S) | 5, 5, 5 |
| tRNAs | 58 |
| ncRNAs | 3 |
| CRISPR arrays | 1 |

Table 2

Functional annotation of genes associated with probiotic properties in *L. paracasei* UCO-100.

Note: Genome assembly and gene statistics are based on the official NCBI Prokaryotic Genome Annotation Pipeline (PGAP) annotation deposited under BioProject PRJNA1482251 and BioSample SAMN61118521. For brevity, locus tags are shown without the AC50GA_ prefix. RefSeq WP accession numbers had not yet been assigned at the time of writing; therefore, locus tags are provided as stable identifiers. Functional predictions were based on protein homology.

| Function | Gene product | Locus tag (AC50GA_) | Contig | Reference RefSeq accession |
|---|---|---|---|---|
| **Adhesion in gastrointestinal tract** | D-alanine–poly(phosphoribitol) ligase subunit DltA | 00650 | 1 | WP_019885987.1 |
| | D-alanyl-lipoteichoic acid biosynthesis protein DltB | 00655 | 1 | WP_010493763.1 |
| | LPXTG cell wall anchor domain-containing protein | 07825 | 6 | WP_011674963.1 |
| | SpaH/EbpB family LPXTG-anchored major pilin | 08735 | 8 | WP_003567305.1 |
| **Autoaggregation / EPS biosynthesis** | Putative polysaccharide biosynthesis protein | 01080 | 1 | WP_003564130.1 |
| **Bacteriocin production** | Blp family class II bacteriocin | 12785 | 17 | WP_016372975.1 |
| | Garvicin Q family class II bacteriocin | 06315 | 4 | WP_016369810.1 |
| | Class IIb bacteriocin | 12790 | 17 | WP_019863230.1 |
| | Bacteriocin immunity protein | 06320 | 4 | WP_016369811.1 |
| | bacteriocin-like peptide, LSEI_2386 family | 08645 | 8 | WP_012491943.1 |
| | peptide cleavage/export ABC transporter | 08650 | 8 | WP_003567347.1 |
| | bacteriocin immunity family protein | 08675 | 8 | WP_003580847.1 |
| | bacteriocin immunity protein | 08680 | 8 | WP_003580845.1 |
| **Enzyme production** | Alpha-galactosidase | 02060 | 1 | WP_013245597.1 |
| | 6-phospho-beta-galactosidase | 14255 | 33 | WP_003589794.1 |

| Function | Gene product | Locus tag (AC50GA_) | Contig | Reference RefSeq accession |
|---|---|---|---|---|
| | Glycoside hydrolase family 1 protein | 04385 | 3 | WP_005715340.1 |
| | Type I methionyl aminopeptidase | 02410 | 1 | WP_003578592.1 |
| | Phosphate acyltransferase PlsX | 03880 | 2 | WP_016382572.1 |
| **Stress response** | Molecular chaperone DnaK | 04130 | 2 | WP_016388828.1 |
| | Molecular chaperone DnaJ | 04135 | 2 | WP_016386604.1 |
| | Cardiolipin synthase | 06460 | 5 | WP_003584308.1 |
| | Hsp20/alpha crystallin family protein | 00155 | 1 | WP_016369515.1 |
| | Hsp33 family molecular chaperone HslO | 11415 | 13 | WP_019885431.1 |
| | Universal stress protein | 04255 | 3 | WP_016371292.1 |

Table 3

**S**afety assessment of *L. paracasei* UCO-100: antibiotic resistance genes, CRISPR-Cas system, mobile genetic elements, virulence genes, and hemolytic activity. The antibiotic panel corresponds to the *L. casei/paracasei* group, as defined by EFSA guidance (EFSA Journal 2025;23(11):9705; adopted September 24, 2025).

Antibiotic resistance genes were predicted using CARD, ResFinder, ARG-ANNOT, and AMRFinderPlus.

CRISPR-Cas systems were predicted using CRISPRCasFinder. Mobile genetic elements were predicted using VRprofile2. Virulence genes were predicted using a curated *Enterococcus*-associated panel and the Virulence Factor Database (VFDB).

| **Antibiotic sensitivity** | | | |
|---|---|---|---|
| **Antibiotics**[a] | | **Potential antibiotic resistance gene**[b] | |
| Ampicillin | | Not detected | |
| Chloramphenicol | | Not detected | |
| Clindamycin | | Not detected | |
| Erythromycin | | Not detected | |
| Gentamicin | | Not detected | |
| Kanamycin | | Not detected | |
| Streptomycin | | Not detected | |
| Tetracycline | | Not detected | |
| Vancomycin | | N/A | |
| **CRISPR**[c] | | | |
| **Location** | **Start** | **End** | **Consensus repeat** |
| Contig 3 | 30,354 | 32,369 | GTCTCAGGTAGATGTCGAATCAATCAGTTCAAGAGC |
| **Orientation** | **Number of repeats** | **Number of spacers** | **Evidence level** |
| Reverse (AT%-based); CRISPRDirection undetermined | 30 | 30 (30 bp each; 1 duplicated) | 4 |
| **Cas**[c] | | | |
| **Location** | **Type of Cas gene** | **Start** | **End** |
| Contig 3 | cas9_TypeII-A | 24,185 | 28,270 |

| Antibiotic sensitivity | | | |
|---|---|---|---|
| **Antibiotics[a]** | | **Potential antibiotic resistance gene[b]** | |
| Contig 3 | cas1_TypeII-A | 28,467 | 29,372 |
| Contig 3 | cas2_TypeII-A | 29,350 | 29,655 |
| Contig 3 | csn2_TypeII-A | 29,652 | 30,329 |
| **Mobile genetic elements[d]** | | | |
| **Contig** | **Type of element** | **Position (bp)** | **Length (bp) / GC content (%)** |
| 3 | Genomic island | 170,558–180,369 | 9,811 / 36.19 |
| 1 | Prophage | 207,183–240,542 | 33,359 / 45.20 |
| 1 | Prophage | 397,031–426,223 | 29,192 / 45.77 |
| 2 | Prophage | 150,315–165,148 | 14,833 / 48.14 |
| 19 | IS cluster/Tn (ISLsa1 / ISLrh2 / ISLho2) | 17,322–25,165 | 7,843 / 44.84 |
| 25 | IS cluster/Tn (IS1310 / IS153) | 7,584–11,939 | 4,355 / 46.13 |
| **Virulence genes[e] (Enterococcus-associated panel)** | | | |
| **Virulence gene** | **Result** | **Virulence gene** | **Result** |
| Gelatinase (gelE) | Not detected | Cytolysin (cylA) | Not detected |
| Hyaluronidase (hyl) | Not detected | Cytotoxin K (cytK) | Not detected |
| Aggregation substance (asa1) | Not detected | Enterotoxin (nhe) | Not detected |

| Antibiotic sensitivity | | | |
|---|---|---|---|
| **Antibiotics[a]** | | **Potential antibiotic resistance gene[b]** | |
| Enterococcal surface protein (esp) | Not detected | Hemolysin (hbl) | Not detected |
| Serine protease (sprE) | Not detected | | |
| **Hemolysis** | | | |
| Type of hemolysis | Gamma | | |

**Tolerance to acidic pH and bile salts.** The number of viable *L. paracasei* UCO-100 cells, expressed as CFU/mL, under simulated gastric conditions is shown in Table 4 and Fig. 2. Strain remained viable and exhibited net growth under the tested acidic and bile conditions. Only a slight decrease in growth was observed at pH 3, with viable counts decreasing from $8 \times 10^7$ CFU/mL in the control to $8 \times 10^6$ CFU/mL in the pH-adjusted culture after 24 h

**Hydrophobicity, autoaggregation, and adhesion to abiotic surfaces.** *L. paracasei* UCO-100 exhibited high hydrophobicity (73.6 ± 1.24%), similar to that observed for the control strain *L. fermentum* UCO-979C (78.67 ± 0.95%). Both strains also showed high adhesion to abiotic surfaces, with 57 bacteria/field for *L. paracasei* UCO-100 and 68 bacteria/field for *L. fermentum* UCO-979C. Regarding autoaggregation, *L. paracasei* UCO-100 showed the ability to aggregate after 24 h of culture (Table 4).

Table 4
Bile salt tolerance, Acid tolerance, autoaggregation, hydrophobicity and adherence ability of *L. paracasei* UCO-100. For growth curve data are shown as means of three independent experiments. Results are expressed in CFU/mL. Control: *L. fermentum* UCO-979C.

| **Bile Salt Tolerance (Oxgall 2%)** | | | | | |
|---|---|---|---|---|---|
| Strain | 0 h | 1 h | 2 h | 3 h | 24 h |
| *L. paracasei* UCO-100 | 2.57x10^5 | 2.1x10^6 | 3.67x10^6 | 1.35x10^7 | 7.17x10^7 |
| Control | 5.3x10^5 | 1.9x10^6 | 3.1x10^6 | 1.2x10^7 | 8.1x10^7 |
| **Acid Tolerance (pH3)** | | | | | |
| Strain | 0 h | 1 h | 2 h | 3 h | 24 h |
| *L. paracasei* UCO-100 | 4.87x10^5 | 1.17x10^6 | 1.6x10^6 | 3.4x10^6 | 8.33x10^6 |
| Control | 5.3x10^5 | 1.9x10^6 | 3.1x10^6 | 1.2x10^7 | 8.1x10^7 |
| **Acid Tolerance (pH5)** | | | | | |
| Strain | 0 h | 1 h | 2 h | 3 h | 24 h |
| *L. paracasei* UCO-100 | 5.53x10^5 | 1.6x10^6 | 2.2x10^6 | 3.73x10^6 | 2.07x10^7 |
| Control | 5.3x10^5 | 1.9x10^6 | 3.1x10^6 | 1.2x10^7 | 8.1x10^7 |
| **Autoaggregation (%)** | | | | | |
| *L. paracasei UCO-100* | | 54.3 ± 1.44 | *L. fermentum* UCO-979C | | 61.05 ± 1.06 |
| **Hydrophobicity (%)** | | | | | |
| *L. paracasei* UCO-100 | | ++ (73.6 ± 1.24) | *L. fermentum* UCO-979C | | ++ (78.67 ± 0.95) |
| **Adherence (bacteria per field)** | | | | | |
| *L. paracasei* UCO-100 | | Strong (57) | *L. fermentum* UCO-979C | | Strong (68) |

**Antibiotic resistance and hemolytic activity.** *L. paracasei* UCO-100 showed susceptibility to the different antibiotics evaluated, as shown in Table 5, according to the criteria established by Georgieva et al. The strain exhibited resistance only to bacitracin, an antibiotic used for topical applications. Regarding hemolytic activity, no hemolysis was detected and the strain exhibited a γ-hemolytic phenotype on blood agar.

Table 5

**Antibiotic susceptibility profile of L. paracasei UCO-100.** Antibiotic susceptibility was classified as resistant (R), moderately susceptible (MS), susceptible (S), or highly susceptible (HS). Amoxicillin/c : Amoxicillin / clavulanic acid; Amp. Sulbactam: Ampicillin/ Sulbactam; Trimethoprim/su: Trimethoprim/ Sulfamethoxazole.

| Antibiotic | Disc conc. (µg) | Diameter (mm) | Result | Antibiotic | Disc conc. (µg) | Diameter (mm) | Result |
|---|---|---|---|---|---|---|---|
| **Nalidixic Acid** | 30 | 8 | MS | **Amikacin** | 30 | 10 | MS |
| **Amoxicillin** | 10 | 24 | S | **Amoxicillin/c** | 30 | 26 | HS |
| **Ampicillin** | 10 | 19 | S | **Amp. Sulbactam** | 20 | 23 | S |
| **Azithromycin** | 15 | 28 | HS | **Bacitracin** | DD | 6 | R |
| **Cefazolin** | 30 | 15 | MS | **Cefotaxime** | 30 | 17 | S |
| **Cefoxitin** | 30 | 16 | MS | **Ceftazidime** | 30 | 9 | MS |
| **Ceftriaxone** | 30 | 10 | MS | **Cefuroxime** | 30 | 22 | S |
| **Ciprofloxacin** | 5 | 18 | S | **Clarithromycin** | 15 | 37 | HS |
| **Clindamycin** | 2 | 32 | HS | **Chloramphenicol** | 30 | 32 | HS |
| **Erythromycin** | 15 | 33 | HS | **Gentamicin** | 10 | 11 | MS |
| **Imipenem** | 15 | 27 | HS | **Kanamycin** | 30 | 10 | MS |
| **Levofloxacin** | 5 | 21 | S | **Metronidazole** | 5 | 8 | MS |
| **Moxifloxacin** | 5 | 25 | S | **Neomycin** | 30 | 20 | S |
| **Nitrofurantoin** | 30 | 19 | S | **Norfloxacin** | 10 | 17 | S |
| **Novobiocin** | 5 | 19 | S | **Optochin** | DD | 16 | MS |
| **Oxacillin** | 1 | 10 | MS | **Penicillin** | 10 | 33 | HS |
| **Trimethoprim/su.** | 25 | 12 | MS | **Tetracycline** | 30 | 41 | HS |
| **Tobramycin** | 10 | 16 | MS | **Vancomycin** | 30 | 8 | MS |

# Discussion

Probiotics are live microorganisms that perform three key functions in the human body: modulation of the immune response, restoration of intestinal microbiota balance, and reinforcement of the gastrointestinal barrier [13]. Therefore, probiotic bacteria must be able to survive under different growth conditions, including those encountered in the gastrointestinal tract, while retaining the ability to grow, colonize, and produce various metabolites in these environments [14].

The draft genome of *L. paracasei* UCO-100 was assembled using a hybrid Nanopore long-read and MGI short-read approach, achieving 269× combined coverage and yielding a 3,007,747 bp genome distributed across 61 contigs (N50 ≈ 167 kb; largest contig 470,112 bp). While this represents a high-quality draft assembly suitable for functional and comparative genomic analyses, it remains fragmented relative to fully closed reference genomes such as *L. paracasei* ATCC 334 or BL23. This fragmentation has direct implications for the interpretation of results presented below and underscores that genome closure should be pursued to fully resolve gene neighborhoods, plasmid content, and mobile genetic elements.

The candidate probiotic strain evaluated in this study belongs to *L. paracasei*, confirmed by its phylogenetic analysis, a species that has been extensively investigated for its probiotic properties and is closely associated with the gastrointestinal tract and fermented products, including kefir and dairy products [5, 6]. Species-level identification of UCO-100 as *L. paracasei* was independently supported by two complementary analyses. Average nucleotide identity (OrthoANIu) against 10 *L. paracasei* reference genomes ranged from 98.23% to 98.45%, including 98.44% against the type strain JCM 8130 (= ATCC 25302), well above the 95–96% species boundary and clearly discontinuous from the ANI observed against *L. rhamnosus* (77.1–77.8%), *L. casei* (77.1–78.4%), and *L. zeae* (77.1–77.9%). This was corroborated by a phylogenomic species tree inferred from 1,622 single-copy orthologous genes (OrthoFinder, STAG/STRIDE), which placed UCO-100 within a well-supported *L. paracasei* clade (STAG support ≥ 0.96) clearly separated from the *L. rhamnosus* and *L. casei*/*L. zeae* clades. Therefore, *L. paracasei* UCO-100 was expected to possess characteristics supporting its potential use as a candidate probiotic strain.

First, the prediction of genes potentially associated with probiotic functions indicated that *L. paracasei* UCO-100 harbors genes related to gastrointestinal adhesion, including genes encoding anchor proteins, intestinal epithelial-binding proteins, and proteins involved in cell surface modification, such as DltA and DltB [15]. Genes encoding adhesins and proteins involved in biofilm formation were also identified, including members of the SpaH/EbpB pilin protein family containing an LPXTG motif [16]. These genomic findings are supported by the adhesion to abiotic surface assay, in which *L. paracasei* UCO-100 showed high adherence, similar to that of the previously studied control strain *L. fermentum* UCO-979C [17]. However, adhesion to the gastrointestinal tract needs to be demonstrated *in vitro*.

Regarding autoaggregation, an important characteristic for colonization and biofilm formation, genes involved in exopolysaccharide (EPS) biosynthesis were identified. EPSs participate in aggregation and confer properties of interest, including protection against stress, competitive exclusion, and immunomodulation [18, 19]. The autoaggregation capacity of the strain was also confirmed experimentally, with *L. paracasei* UCO-100 reaching 54.3% autoaggregation after 24 h (Table 4). This value was comparable to that of the control strain *L. fermentum* UCO-979C, which has previously been shown to be a biofilm-forming strain in the intestine [19].

Concerning bacteriocin production, genomic prediction identified two contigs containing putative genes associated with this process (Fig. 1D, Table 2). The cluster located on contig 8 (146,905 bp) displayed the most complete architecture, including a bacteriocin-like peptide belonging to the LSEI_2386 family, an

upstream two-component regulatory system (LytR/AlgR and a GHKL histidine kinase), a dedicated ABC transporter containing a peptidase domain for peptide processing and export, classified by antiSMASH as a “core biosynthetic” gene, an accessory secretion protein, and two downstream immunity proteins. Thus, this cluster seems to contain the four functional modules typically found in a complete class II bacteriocin system: regulation, synthesis, transport, and immunity [20]. However, only the ABC transporter was automatically recognized as a “core biosynthetic” gene according to the antiSMASH detection rules, whereas the regulatory, accessory transport, and immunity functions were inferred from PGAP homology-based functional annotation.

The cluster located on contig 17 (37,426 bp) contains two adjacent structural genes—a Blp family peptide and a class IIb bacteriocin—classified as “core biosynthetic” genes. These genes are flanked by enzymes, including oxidoreductases, a sugar acetyltransferase, and two CPBP-family intramembrane endopeptidases, which were classified by antiSMASH as “additional biosynthetic” genes, as well as an immunity protein [20].

It is worth noting that the first gene of the contig 8 cluster (locus_tag08625) begins at position 1 of its contig, coinciding exactly with the contig boundary. This raises the possibility that additional upstream sequence, potentially including further regulatory or accessory genes, was not captured due to assembly fragmentation, and that the true extent of this cluster may be underestimated. Similarly, the contig 17 cluster ends only 1,665 bp from its contig’s terminus, leaving comparatively little flanking sequence on that side. These observations are consistent with the fragmented nature of the current UCO-100 assembly (61 contigs) and emphasize that cluster boundaries reported here should be interpreted as provisional pending genome closure.

Neither cluster showed significant matches to characterized clusters in the MIBiG database using KnownClusterBlast, suggesting that they represent previously undescribed architectures, although the individual genes showed clear homology to known bacteriocin families based on PGAP/RefSeq annotation.

It is important to note that a third gene, annotated by PGAP as garvicin Q (class II bacteriocin family, contig 4), was not identified as an independent biosynthetic cluster by antiSMASH, even under relaxed detection criteria. Its immediate genomic context did not meet the detection rules of the tool; therefore, its status as a functional cluster remains independently unconfirmed. Overall, these findings predict that *L. paracasei* UCO-100 may produce bacteriocins whose functionality and activity against pathogens require experimental confirmation. Among the predicted clusters, the cluster located on contig 8 appears particularly relevant because of the presence of the complete predicted architecture [20].

Regarding the synthesis of enzymes associated with probiotic properties, genomic prediction indicated that the strain harbors genes encoding α- and β-galactosidases, which participate in lactose processing, may improve the digestion of dairy-derived compounds, and may contribute to reducing intestinal gas production [21, 22]. In addition, genes encoding enzymes involved in metabolic processes associated with

efficient carbon utilization, prebiotic utilization, metabolic adaptation, and energy generation were identified [23, 24].

Respecting the stress response, several genes involved in this process were predicted, including those encoding the DnaK and DnaJ chaperones, which contribute to maintaining cellular stability and prolonging survival [25]. Genes encoding heat shock proteins (Hsps), universal stress proteins, and cardiolipin synthase were also identified. These proteins participate in responses to oxidative stress and resistance to bile salts, temperature changes, and acidic pH [26, 27]. These genomic findings are consistent with the experimental results, in which *L. paracasei* UCO-100 was able to grow and maintain its viability at acidic pH values (pH 3 and 5) and in the presence of bile salts (Fig. 2). Tolerance to acid and bile salts is a desirable characteristic in human probiotic bacteria, due to the stressful conditions found in the gastrointestinal tract, so tolerance to an acidic pH like pH3 is important for colonizing the gastric mucosa layer.

About probiotic safety, the predictive analysis based on the EFSA (European Food Safety Authority) panel indicated that the strain does not harbor genes associated with antibiotic resistance of relevance to probiotic strains [28]. This finding was supported by the antibiotic disc inhibition assay, in which the strain was evaluated against 36 different antibiotics and was susceptible to most of them. Resistance was observed only to bacitracin, which corresponds to an intrinsic resistance and does not represent a risk of transfer to other bacteria [29].

No virulence genes associated with the strain were identified either using the curated Enterococcus-associated panel or through the complementary genome-wide BLAST-based screening against the VFDB core dataset. It should be noted that no *Lactobacillus*-specific virulence factor database is currently available; therefore, screening relied on the general VDFB core dataset and the classical *Enterococcus*-associated panel, which may not fully capture virulence determinants relevant to lactobacilli. Hemolytic activity was determined phenotypically, showing a γ-hemolytic (non-hemolytic) phenotype, consistent with the absence of hemolysin-related virulence genes in the genome.

Genes associated with three prophages, one genomic island, and two insertion sequences were identified, suggesting evolutionary processes or adaptability of the strain; no antibiotic resistance genes were detected within any of these mobile genetic elements, indicating that their presence does not represent a probiotic safety risk [30]. In addition, prophages may confer characteristics relevant to interactions with certain pathogens. Further studies are therefore required to determine whether these prophages are complete, inducible, or functional.

Finally, CRISPR analysis identified a putative Type II-A CRISPR-Cas system on contig 3 (231,472 bp), comprising the core *cas* genes (*cas9*, *cas1*, *cas2*, *csn2*) together with a CRISPR array of 30 direct repeats (36 bp) and 29 spacers (30 bp each). This finding suggests that UCO-100 possesses an active adaptive immune mechanism against exogenous mobile genetic elements such as bacteriophages and plasmids, potentially contributing to its genomic stability, although its functional activity and contribution to genome stability remain to be experimentally determined [31].

Taken together, the genomic predictions for *L. paracasei* UCO-100 and the corresponding experimental findings indicate that this strain possesses favorable characteristics associated with probiotic potential, particularly regarding its safety profile. In addition, the prediction of genes associated with probiotic properties supports its consideration as a potential probiotic strain and warrants further investigation of specific functions that may provide benefits to the h

# Conclusions

The genomic analysis of *L. paracasei* UCO-100 revealed a set of characteristics supporting its potential as a probiotic strain. The identification of functional genes associated with intestinal epithelial adhesion, exopolysaccharide biosynthesis, carbohydrate metabolism, and stress response suggests that the strain possesses mechanisms that favor its survival, persistence, and functional activity in the gastrointestinal tract. Likewise, the detection of RiPP-like biosynthetic gene clusters and genes associated with bacteriocin production further supports its potential to exert antagonistic activity against pathogenic microorganisms. In addition, the presence of a CRISPR-Cas system indicates a defense mechanism against exogenous DNA that could contribute to the genetic stability and safety of the strain. Finally, although mobile genetic elements, including genomic islands, prophages, and insertion sequences, were identified, these primarily represent evidence of genomic plasticity and evolutionary adaptation and, in the absence of clinically relevant virulence or acquired resistance genes, do not compromise the safety profile of the strain. Taking together, these findings provide strong genomic evidence supporting the potential of *L. paracasei* UCO-100 for probiotic applications.

# Methods

**Isolation and culture conditions of L. paracasei UCO-100.** The UCO-100 strain was isolated from a human gastric corpus biopsy in 2006. *L. paracasei* UCO-100 was obtained from the culture collection of the Bacterial Pathogenicity Laboratory at the Universidad de Concepción and cultured according to established laboratory protocols. Briefly, the strain was cultured on Man, Rogosa and Sharpe (MRS) (BD Difco™, Franklin Lakes, NJ, USA) agar and incubated at 37°C under 10% $CO_2$ for 24 h. After incubation, two to three colonies were transferred to MRS broth (BD Difco™, Franklin Lakes, NJ, USA) and incubated under the same conditions described above to obtain cultures for subsequent assays.

**Genomic DNA extraction and genome análisis**. *L. paracasei* UCO-100 was cultured in MRS broth at 37°C for 24 h under microaerophilic conditions. Genomic DNA was extracted from the harvested cells using the GeneJET Genomic DNA Purification Kit (Thermo Fisher Scientific, Waltham, MA, USA) according to the manufacturer's instructions, with cells subjected to mechanical disruption followed by enzymatic lysis using lysozyme (50 mg $mL^{-1}$) and proteinase K (20 mg $mL^{-1}$). Genomic DNA concentration was determined using a Qubit 4.0 fluorometer (Thermo Fisher Scientific) with the Qubit dsDNA HS Assay Kit, and DNA integrity was evaluated by electrophoresis on a 1.5% agarose gel. Only DNA samples meeting the quality requirements were used for whole-genome sequencing.

## Whole-genome sequencing, assembly, and annotation

A hybrid sequencing strategy combining short- and long-read technologies was used. For short-read sequencing, a genomic library was prepared from 100 ng of genomic DNA (gDNA) using the MGIEasy FS DNA Library Prep Set (MGI Tech, Shenzhen, China), following the manufacturer's instructions. Library preparation comprised DNA fragmentation, end repair and adapter ligation, purification, single-strand separation and circularization, and DNA nanoball (DNB) synthesis. The library was sequenced on a DNBSEQ-G400 platform (MGI Tech, Shenzhen, China) using DNBSEQ technology, generating 150-bp paired-end (PE150) reads.

For long-read sequencing, high-molecular-weight genomic DNA was extracted using a DNA extraction kit. Libraries were prepared using the Ligation Sequencing Kit V14 (SQK-LSK114; Oxford Nanopore Technologies, Oxford, UK) and sequenced on a MinION device (Oxford Nanopore Technologies, Oxford, UK) using an R10.4.1 flow cell.

De novo hybrid assembly of short and long-read data was performed using Unicycler v0.5.1, yielding a mean genome coverage of 269×. The final assembly comprised 61 contigs with a total length of 3,007,747 bp (largest contig, 470,112 bp; N50, 167,707 bp; L50, 6) and an overall GC content of 46.34%, with no ambiguous bases (N's) in the assembly. Genome annotation was performed using the NCBI Prokaryotic Genome Annotation Pipeline (PGAP) through the GenBank submission workflow.

**Phylogenetic analysis based on orthologous genes and comparison of average nucleotide identity.** Phylogenetic relationships of UCO-100 were constructed based on ortholog gene sequences. Protein sequences for the 17 reference genomes of the *L. casei* group (*L. paracasei*, n = 10; *L. rhamnosus*, n = 4; *L. casei*, n = 2; *L. zeae*, n = 1; accession numbers listed in table S_X) were downloaded from the NCBI website; for UCO-100, PGAP-predicted proteins were used directly. Ortholog analysis was performed using OrthoFinder v2.5.5 [32] and the species tree was inferred using the STAG algorithm and rooted using the STRIDE algorithm in OrthoFinder. The species tree was illustrated using MEGA12. Average Nucleotide Identity (ANI) among the same 18 genomes was calculated using the OrthoANIu algorithm [33] via the EzBioCloud ANI calculator (https://www.ezbiocloud.net/tools/ani; results listed in table S_X). The ANI heatmap was visualized using Matplotlib.

**Acid pH and bile salt tolerance**. The tolerance of *L. paracasei* UCO-100 to acidic pH was evaluated. Briefly, 100 µL of a 24-h liquid culture of UCO-100 or control strains grown in MRS broth was inoculated into 10 mL of MRS broth adjusted to pH 3 or 5 and incubated at 37°C under 10% $CO_2$. Aliquots were collected at 0, 1, 2, 3, and 24 h of incubation to determine viable bacterial counts using the drop plate method. At each time point, 100 µL aliquots were collected and serially diluted to $10^{-5}$. Three 10-µL drops from each prepared dilution were plated onto MRS agar plates, which were subsequently incubated for 24 h at 37°C under 10% $CO_2$.

Bile salt tolerance was evaluated using a similar assay. For this purpose, MRS broth was supplemented with 2% Oxgall bile salts and incubated under the conditions described above, with bacterial viability

evaluated at the same point. Strains that maintained viable counts or the ability to grow in the presence of bile salts were considered tolerant [17].

**Hydrophobicity and autoaggregation analysis.** Hydrophobicity was evaluated using the microbial adhesion to hydrocarbons (MATH) assay. For this purpose, *L. paracasei* UCO-100 and the control strain (*L. fermentum* UCO-979C) were grown in MRS broth for 24 h. Subsequently, the cultures were centrifuged at 5000 × g for 5 min to obtain the bacterial pellet, which was resuspended in phosphate-buffered saline (PBS) to an $OD_{600}$ of 0.4–0.6. A 1.2-mL aliquot of the bacterial suspension was mixed with 0.3 mL of xylene, vortexed for 2 min, and incubated for 10 min at 25°C. The aqueous phase was separated, and the $OD_{600}$ was measured [17]. The percentage of hydrophobicity was calculated according to the criteria of Ocaña et al., and the strain was classified as highly hydrophobic (%H: 71–100, ++), moderately hydrophobic (%H: 36–70, +), or weakly hydrophobic (%H: 0–35), using the following equation:

$$Hydrophobicity\ \ (\%)\ = \frac{Ai\ -\ Af}{Ai}\ x\ 100$$

Where $Ai$ represents the initial absorbance and $Af$ represents the absorbance measured after 10 min of incubation with xylene.

To evaluate the autoaggregation of *L. paracasei* UCO-100, the bacterial suspension adjusted to an $OD_{600}$ of 0.4–0.6 in PBS was allowed to stand and incubated for 24 h at 37°C. Absorbance was measured at $OD_{600}$ after 24 h. Auto-aggregation was calculated using the following equation:

$$Autoaggregation\,(\%)\ = \frac{Ai\ -\ Af}{Ai}\ x\ 100$$

where $\varvec{Ai}$ represents the initial absorbance and $\varvec{Af}$ represents the absorbance of the supernatant after 24 h [34]

**Adhesion to glass surfaces.** *L. paracasei* UCO-100 and the control strain (*L. fermentum* UCO-979C) were grown in MRS broth for 24 h at 37°C under 10% $CO_2$. The bacterial cells were collected by centrifugation and resuspended in 20 mL of MRS broth to a cell density corresponding to McFarland standard No. 2, followed by incubation for 1 h under the conditions described above. Sterile glass slides were immersed in the cultures and incubated for 4 h. After incubation, the slides were subjected to simple staining with crystal violet for 5 min, washed, and allowed to dry at room temperature for 10 min. The samples were examined by microscopy using a 100× objective. Strains were classified as non-adherent (< 20 bacteria per field), moderately adherent (20–50 bacteria per field), or strongly adherent (> 50 bacteria per field) [17].

**Antibiotic susceptibility and hemolytic activity** The susceptibility of *L. paracasei* UCO-100 to different antibiotics was determined using an agar disk diffusion assay with commercial antibiotic discs, according to the protocol described by Garcia et al. [17]. Briefly, a bacterial lawn was prepared from a UCO-100 culture at a concentration of $10^7$, and the different antibiotic disks were subsequently placed on the agar

surface. The plates were incubated for 48 h, after which the diameters of the inhibition zones around the disks were measured. Antibiotic susceptibility was classified according to the criteria of Georgieva et al. [35] as resistant (R), moderately susceptible (MS), susceptible (S),highly susceptible (HS), or not determined (nd).

Hemolytic activity was evaluated by culturing *L. paracasei* UCO-100 in MRS broth for 24 h at 37°C under 10% $CO_2$. Following incubation, the strain was inoculated onto blood agar plates using the lawn culture technique and incubated for 24 h under the same conditions. The presence or absence of hemolysis on the plates was evaluated.

**Genomic safety analysis.** Antibiotic resistance genes were screened by comparison against the Comprehensive Antibiotic Resistance Database [36], ResFinder [37], and ARG-ANNOT [38] using BLAST, as well as using AMRFinderPlus [39], as implemented through the Bakta [40] and NCBI Prokaryotic Genome Annotation Pipeline (PGAP) annotation workflows. The antibiotic panel used in Table 3 were those defined for the *L. casei/paracasei* group in the EFSA guidance on the characterisation of microorganisms in support of the risk assessment of products used in the food chain [28].

Virulence genes were screened against a curated panel of *Enterococcus*-associated virulence factors (*gelE, hyl, asa1, esp, sprE, cylA, cytK, nhe, hbl*) by gene-name matching in the PGAP annotation and, complementarily, against the complete genome sequence using the core dataset of the Virulence Factor Database [41], via the VFDB BLASTX web interface (http://www.mgc.ac.cn/VFs/) and via ABRicate v1.0.1 (Seemann, https://github.com/tseemann/abricate) with BLASTN, applying minimum identity and coverage thresholds of 80%.

CRISPR-Cas systems were identified using CRISPRCasFinder v4.2.20 (Couvin et al., 2018). Plasmid replicons were screened using PlasmidFinder [42] on the official Center for Genomic Epidemiology server (https://cge.food.dtu.dk/services/PlasmidFinder/) using the Gram-positive replicon database with default thresholds (95% identity, 60% coverage). Additional mobile genetic elements (prophages, insertion sequence clusters/transposons, and genomic islands) were predicted using VRprofile2 [43], which integrates the PLSDB, PHASTER, PAIDB, ICEberg, and TnRegistry databases.

# Declarations

**Funding:**

The author received no funding for this work.

**Acknowledgements**

Molecular Biotechnology Doctoral Program and the Laboratory of Bacterial Pathogenicity of the Department of Microbiology, both belonging to the Faculty of Biological Sciences, Universidad de Concepción.

**Author contributions statement**

V.F.B., C.G., and C.P.S. contributed conceptualization of investigation. V.F.B., C.G., C.P.S and H.V.N. analyzed and performed experiments. K.S.-A., M.A. contributed data validation and curation. A.P.G. and M.A. supervised the works. V.F.B. wrote original draft and all authors reviewed and revised manuscript before submission.

**Competing interests**

The authors declare no competing interes

# Data Availability

This Whole Genome Shotgun project has been deposited at DDBJ/ENA/GenBank under the accession JCANKF000000000. The version described in this paper is version JCANKF010000000.

# References


1. Bintsis, T. Lactic acid bacteria as starter cultures: An update in their metabolism and genetics. *AIMS microbiol.* **4** (4), 665–684. https://doi.org/10.3934/microbiol.2018.4.665 (2018).
2. Chen, Y., Zhou, J. & Wang, L. Role and mechanism of gut microbiota in human disease. *Front. Cell. Infect. Microbiol.* **11**, 625913. https://doi.org/10.3389/fcimb.2021.625913 (2021).
3. Valdes, A., Walter, J., Segal, E. & Spector, T. Role of the gut microbiota in nutrition and health. *BMJ* **361**, k2179. https://doi.org/10.1136/bmj.k2179 (2018).
4. Valdebenito-Navarrete, H. et al. Can Probiotics, Particularly *Limosilactobacillus fermentum* UCO-979C and *Lacticaseibacillus rhamnosus* UCO-25A, Be Preventive Alternatives against SARS-CoV-2? *Biology* **12** (3), 384. https://doi.org/10.3390/biology12030384 (2023).
5. Chen, C. T., Chao, W. Y., Lin, C. H., Shih, T. W. & Pan, T. M. Comprehensive Safety Assessment of *Lacticaseibacillus paracasei* subsp. *paracasei* NTU 101 Through Integrated Genotypic and Phenotypic Analysis. *Curr. Issues Mol. Biol.* **46** (11), 12354–12374. https://doi.org/10.3390/cimb46110734 (2024).
6. Abitayeva, G., Kurmangali, D., Baikonys, T. & Bekshin, Z. *Lacticaseibacillus paracasei* subsp. *paracasei* 2LB: Identification of Genes to Assess the Safety and Probiotic Potential of the Strain. *Foods* **14** (19), 3449. https://doi.org/10.3390/foods14193449 (2025).
7. Curry, B. & Crow, V. *LACTOBACILLUS* spp. | *Lactobacillus casei* Group. *Encycl. Dairy Sci.*, 1488–1494, (2002). https://doi.org/10.1016/B0-12-227235-8/00240-6
8. Alizadeh Behbahani, B., Jooyandeh, H., Taki, M. & Falah, F. Evaluation of the probiotic, anti-bacterial, anti-biofilm, and safety properties of *Lacticaseibacillus paracasei* B31-2, *LWT*, (207), 116676. (2024). https://doi.org/10.1016/j.lwt.2024.116676

9. Ana, A. et al. Impact of growth temperature on exopolysaccharide production and probiotic properties of *Lactobacillus paracasei* strains isolated from kefir grains. *Food Microbiol.* **69**, 212–218. https://doi.org/10.1016/j.fm.2017.08.012 (2018).
10. Romero-Luna, H. E. et al. Probiotic Potential of *Lactobacillus paracasei* CT12 Isolated from Water Kefir Grains (Tibicos). *Curr. Microbiol.* **77**, 2584–2592. https://doi.org/10.1007/s00284-020-02016-0 (2020).
11. Liu, C. F. et al. Immunomodulatory and antioxidant potential of *Lactobacillus* exopolysaccharides. *J. Sci. Food Agric.* **91**, 2284–2291. https://doi.org/10.1002/jsfa.4456 (2011).
12. Rossoni, R. D. et al. The Postbiotic Activity of *Lactobacillus paracasei* 28.4 Against Candida auris. *Front. Cell. Infect. Microbiol.* **10**, 397. https://doi.org/10.3389/fcimb.2020.00397 (2020).
13. Vergara Nieto, A. et al. Molecular pathways and clinical applications of probiotics as effective supporters of intestinal, neurologic, and cardiovascular health: A narrative review. *J. Nutr. Biochem.* **157**, 0955–2863. https://doi.org/10.1016/j.jnutbio.2026.110424 (2026).
14. Govaert, M. et al. Survival of Probiotic Bacterial Cells in the Upper Gastrointestinal Tract and the Effect of the Surviving Population on the Colonic Microbial Community Activity and Composition. *Nutrients* **16** (16), 2791. https://doi.org/10.3390/nu16162791 (2024).
15. Nikolopoulos, N. et al. DltC acts as an interaction hub for AcpS, DltA and DltB in the teichoic acid D-alanylation pathway of Lactiplantibacillus plantarum. *Sci. Rep.* **12** (1), 13133. https://doi.org/10.1038/s41598-022-17434-2 (2022).
16. Zheng, K. et al. The Role of LPxTG Motif Proteins in Lactic Acid Bacteria: Unveiling Key Domains for Adhesion and Biofilm Formation. *J. Agric. Food Chem.* **74** (17), 13368–13384. https://doi.org/10.1021/acs.jafc.5c17767 (2026).
17. Apolinaria García, K. et al. Carlos González, Characterization of *Lactobacillus fermentum* UCO-979C, a probiotic strain with a potent anti-*Helicobacter pylori* activity. *Electron. J. Biotechnol.* **25**, 75–83. https://doi.org/10.1016/j.ejbt.2016.11.008 (2017).
18. Ciszek-Lenda, M., Nowak, B., Sróttek, M., Gamian, A. & Marcinkiewicz, J. Immunoregulatory potential of exopolysaccharide from *Lactobacillus rhamnosus* KL37: effects on the production of inflammatory mediators by mouse macrophages. *Int. J. Exp. Pathol.* **92** (6), 382–391. https://doi.org/10.1111/j.1365-2613.2011.00788.x (2011).
19. Garcia-Castillo, V. et al. The Exopolysaccharide of *Lactobacillus fermentum* UCO-979C Is Partially Involved in Its Immunomodulatory Effect and Its Ability to Improve the Resistance against *Helicobacter pylori* Infection. *Microorganisms* **8** (4), 479. 10.3390/microorganisms8040479 (2020). Published 2020 Mar 27.
20. Solis-Balandra, M. A. & Sanchez-Salas, J. L. Classification and Multi-Functional Use of Bacteriocins in Health, Biotechnology, and Food Industry. *Antibiotics* **13** (7), 666. https://doi.org/10.3390/antibiotics13070666 (2024).
21. Zhao, R. et al. A novel α-galactosidase from the thermophilic probiotic *Bacillus coagulans* with remarkable protease-resistance and high hydrolytic activity. *PloS one*. **13** (5), e0197067.

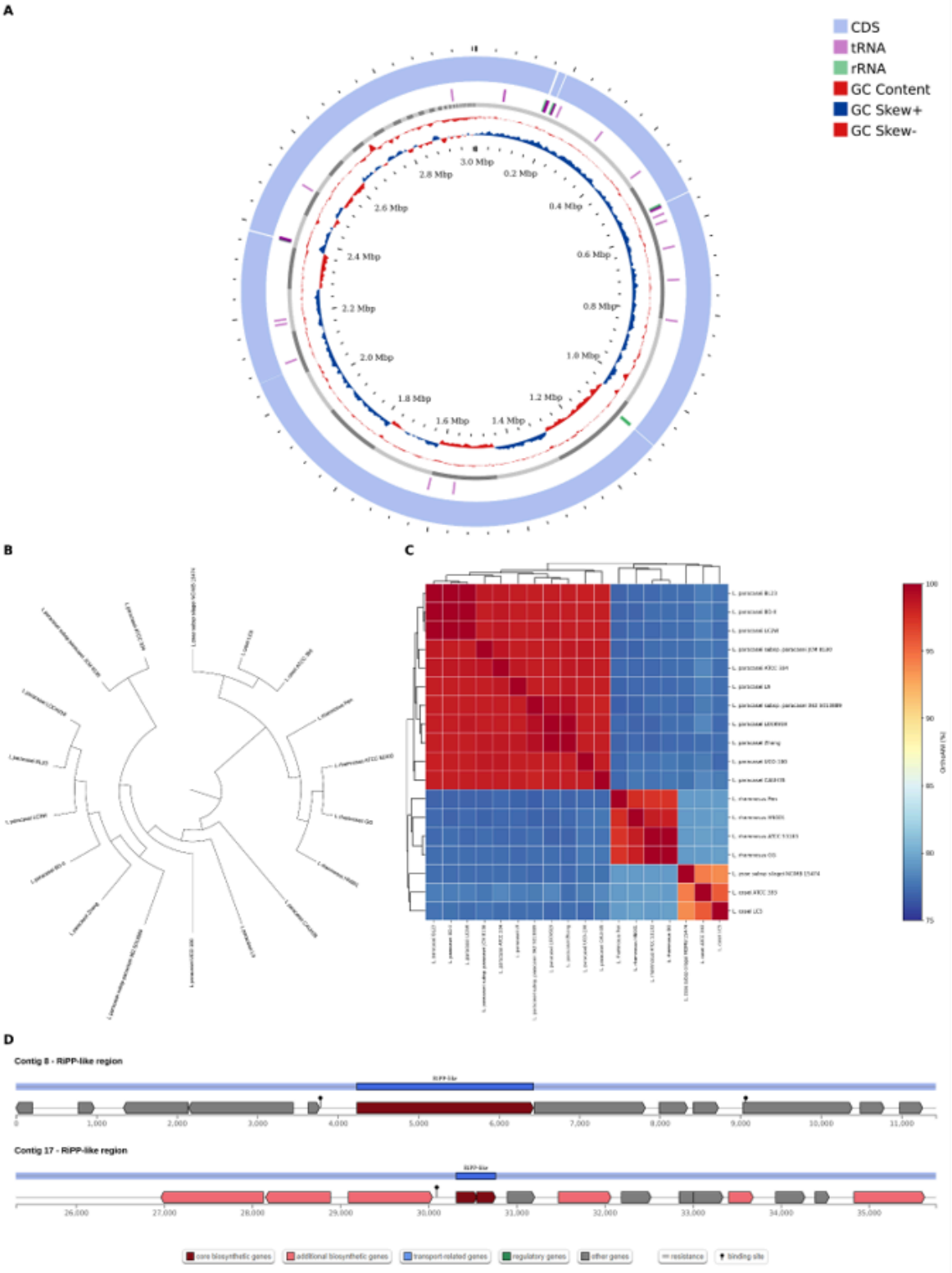
https://doi.org/10.1371/journal.pone.0197067 (2018).

22. Carević, M. et al. Evaluation of β-galactosidase from *Lactobacillus acidophilus* as biocatalyst for galacto-oligosaccharides synthesis: Product structural characterization and enzyme immobilization. *J. Biosci. Bioeng.* **126** (6), 697–704. https://doi.org/10.1016/j.jbiosc.2018.06.003 (2018).
23. Ku, S. Finding and Producing Probiotic Glycosylases for the Biocatalysis of Ginsenosides: A Mini Review. *Molecules* **21** (5), 645. https://doi.org/10.3390/molecules21050645 (2016).
24. Rahman, M. M. et al. Genomic insights into the probiotic potential and genes linked to gallic acid metabolism in *Pediococcus pentosaceus* MBBL6 isolated from healthy cow milk. *PloS one*. **19** (12), e0316270. https://doi.org/10.1371/journal.pone.0316270 (2024).
25. Srinivasan, S. R., Gillies, A. T., Chang, L., Thompson, A. D. & Gestwicki, J. E. Molecular chaperones DnaK and DnaJ share predicted binding sites on most proteins in the *E. coli* proteome. *Mol. Biosyst*. **8** (9), 2323–2333. https://doi.org/10.1039/c2mb25145k (2012).
26. Schnizlein, M. et al. Non-redundant cardiolipin synthases shape lipid composition and stress resilience in *Bacteroides fragilis*. *bioRxiv*, 2025.05.12.653583. (2025). https://doi.org/10.1101/2025.05.12.653583
27. Mills, S., Stanton, C., Fitzgerald, G. F. & Ross, R. P. Enhancing the stress responses of probiotics for a lifestyle from gut to product and back again. *Microb. Cell. Fact.* **10** (Suppl 1). https://doi.org/10.1186/1475-2859-10-S1-S19 (2011)., S19 DOI.
28. Committee, E. F. S. A. S. et al. Guidance on the characterisation of microorganisms in support of the risk assessment of products used in the food chain. *EFSA J.* **23** (11), e9705. https://doi.org/10.2903/j.efsa.2025.9705 (2025).
29. Mohamad, M., Hurst, M. M., Elkrewi, E., Randall, C. P. & O'Neill, A. J. Nature of bacitracin resistance in *Staphylococcus aureus*. *Antimicrob. Agents Chemother.* **69** (12), e0087525. https://doi.org/10.1128/aac.00875-25 (2025).
30. Johnson, B. R. & Klaenhammer, T. R. Impact of genomics on the field of probiotic research: historical perspectives to modern paradigms. *Antonie van Leeuwenhoek*. **106** (1), 141–156. https://doi.org/10.1007/s10482-014-0171-y (2024).
31. Hussain, A. et al. Exploring the emerging role of CRISPR-Cas systems in probiotic development, *Eng Microbiol*, (6) 3, 100279, ISSN 2667–3703, (2026). https://doi.org/10.1016/j.engmic.2026.100279
32. Emms, D. M. & Kelly, S. OrthoFinder: phylogenetic orthology inference for comparative genomics. *Genome Biol.* **20**, 238. https://doi.org/10.1186/s13059-019-1832-y (2019).
33. Yoon, S. H. et al. A large-scale evaluation of algorithms to calculate average nucleotide identity. *Antonie van Leeuwenhoek*. **110**, 1281–1286. https://doi.org/10.1007/s10482-017-0844-4 (2017).
34. Bae, W. Y. et al. Draft genome sequence and probiotic functional property analysis of *Lactobacillus gasseri* LM1065 for food industry applications. *Sci. Rep.* **13**, 12212. https://doi.org/10.1038/s41598-023-39454-2 (2023).
35. Georgieva, R. N. et al. Identification and *in vitro* characterisation of *Lactobacillus plantarum* strains from artisanal Bulgarian white brined cheeses. *J. basic. microbiol.* **48** (4), 234–244.

https://doi.org/10.1002/jobm.200700355 (2008).

36. Alcock, B., Raphenya, A., Lau, T., Tsang, K. & Bouchard, M. *et. al*. CARD 2020: antibiotic resistome surveillance with the comprehensive antibiotic resistance database, *Nucleic Acids Research*, (48), Issue D1, D517–D525, (2020). https://doi.org/10.1093/nar/gkz935
37. Bortolaia, V. et al. ResFinder 4.0 for predictions of phenotypes from genotypes. *J. Antimicrob. Chemother.* **75** (Issue 12), 3491–3500. https://doi.org/10.1093/jac/dkaa345 (2020).
38. Gupta, S. K. et al. ARG-ANNOT, a new bioinformatic tool to discover antibiotic resistance genes in bacterial genomes. *Antimicrob. agents chemother.* **58** (1), 212–220. https://doi.org/10.1128/AAC.01310-13 (2014).
39. Feldgarden, M. et al. AMRFinderPlus and the Reference Gene Catalog facilitate examination of the genomic links among antimicrobial resistance, stress response, and virulence. *Sci. Rep.* **11**, 12728. https://doi.org/10.1038/s41598-021-91456-0 (2021).
40. Schwengers, O. et al. Bakta: rapid and standardized annotation of bacterial genomes via alignment-free sequence identification. *Microb. genom*. **7** (11), 000685. https://doi.org/10.1099/mgen.0.000685 (2021).
41. Liu, B., Zheng, D., Zhou, S., Chen, L. & Yang, J. VFDB : a general classification scheme for bacterial virulence factors, *Nucleic Acids Researc*h, (50), Issue D1, D912–D917, (2022). https://doi.org/10.1093/nar/gkab1107 (2022).
42. D.Couvin, A., Bernheim, C., Toffano-Nioche, M., Touchon, J. & Michalik *et. al*, CRISPRCasFinder, an update of CRISRFinder, includes a portable version, enhanced performance and integrates search for Cas proteins, *Nucleic Acids Research*, (46), Issue W1, W246–W251, (2018). https://doi.org/10.1093/nar/gky425
43. Wang, M. et al. VRprofile2: detection of antibiotic resistance-associated mobilome in bacterial pathogens, *Nucleic Acids Research*, (50), Issue W1, W768–W773, (2022). https://doi.org/10.1093/nar/gkac321
44. Blin, K. et al. antiSMASH 8.0: extended gene cluster detection capabilities and analyses of chemistry, enzymology, and regulation. *Nucleic Acids Res.* **53** (W1), W32–W38. https://doi.org/10.1093/nar/gkaf334 (2025).
45. Terlouw, B. R. et al. MIBiG 3.0: a community-driven effort to annotate experimentally validated biosynthetic gene clusters. *Nucleic Acids Res.* **51** (D1), D603–D610. https://doi.org/10.1093/nar/gkac1049 (2023).

# Figures




## Figure 1

Genomic and functional characterization of *L. paracasei* UCO-100. (A) Circular genome map of the 61 contigs comprising the 3,007,747-bp draft genome assembly. Tracks from outside to inside represent coding sequences (CDSs), tRNA genes, rRNA genes, contigs, GC content, and GC skew. (B) Phylogenetic tree showing the relationship of *L. paracasei*UCO-100 with the analyzed strains. (C) Average nucleotide identity (OrthoANIu) heatmap of the same 18 genomes. (D) Bacteriocin (RiPP-like) biosynthetic gene

clusters identified using antiSMASH 8.0.4. Genes are colored according to the antiSMASH gene classification (core biosynthetic, additional biosynthetic, and other), while black markers (•) indicate predicted regulatory binding sites.

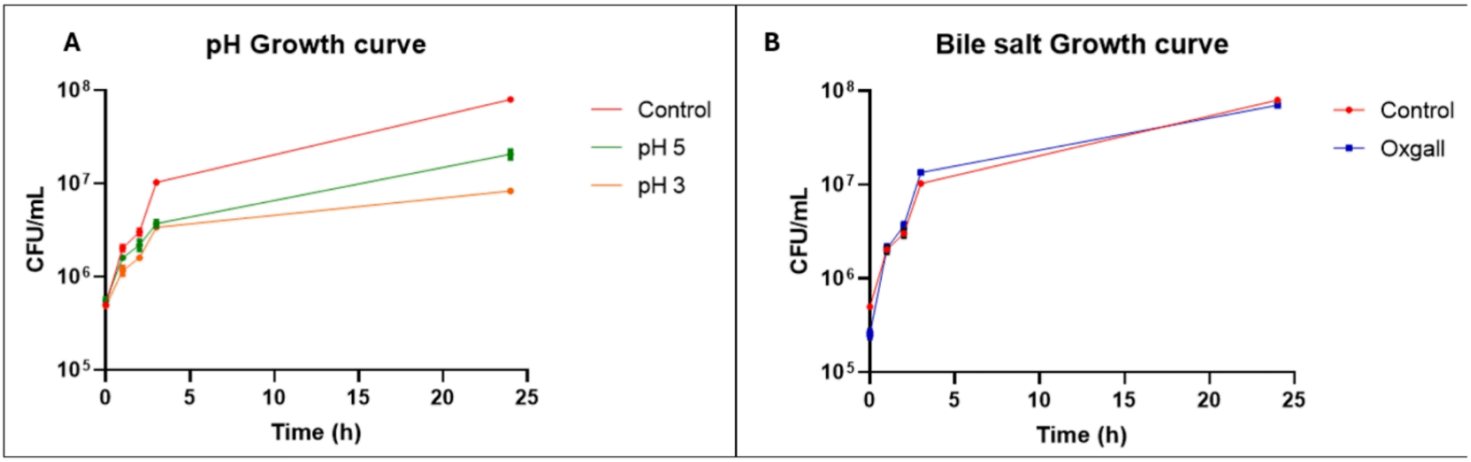



**Figure 2**

**Growth of *L. paracasei* UCO-100 under acidic pH and bile salt conditions.** (A) Growth in MRS medium adjusted to pH 3 (orange) and pH 5 (green). (B) Growth in MRS medium supplemented with Oxgall (blue). Growth in MRS medium alone (red) was used as the control. Growth was evaluated over 24 h, and viable cell counts are expressed as CFU/mL. pH: One-way ANOVA, F 0.8994, P value 0.4326, ns ($P < 0.05$), Bile salt: t test, $P$ value 0.9541, ns ($P< 0.05$)